AGU PUBLICATIONS

JGR

Journal of Geophysical Research: Atmospheres

RESEARCH ARTICLE

10.1002/2015JD023319

# Satellite estimates of precipitation susceptibility in low-level marine stratiform clouds

**C. R. Terai[1,2], R. Wood[1], and T. L. Kubar[3]**

[1]Department of Atmospheric Sciences, University of Washington, Seattle, Washington, USA, [2]Department of Atmospheric Science, Colorado State University, Fort Collins, Colorado, USA, [3]Program for Climate Model Diagnosis and Intercomparison, Lawrence Livermore National Laboratory, Livermore, California, USA

**Key Points:**
- Precipitation susceptibility varies with liquid water path (LWP) and drop number concentration (N)
- Regional differences in susceptibility cannot be explained by LWP and N distributions
- Results suggest additional controls on precipitation, beyond LWP and N, which control susceptibility

**Correspondence to:**
C. R. Terai,
terai1@llnl.gov

**Citation:**
Terai, C. R., R. Wood, and T. L. Kubar (2015), Satellite estimates of precipitation susceptibility in low-level marine stratiform clouds, *J. Geophys. Res. Atmos.*, *120*, doi:10.1002/2015JD023319.

Received 9 MAR 2015
Accepted 28 JUL 2015
Accepted article online 31 JUL 2015

**Abstract** Quantifying the sensitivity of warm rain to aerosols is important for constraining climate model estimates of aerosol indirect effects. In this study, the precipitation sensitivity to cloud droplet number concentration ($N_d$) in satellite retrievals is quantified by applying the precipitation susceptibility metric to a combined CloudSat/Moderate Resolution Imaging Spectroradiometer data set of stratus and stratocumulus clouds that cover the tropical and subtropical Pacific Ocean and Gulf of Mexico. Consistent with previous observational studies of marine stratocumulus, precipitation susceptibility decreases with increasing liquid water path (LWP), and the susceptibility of the mean precipitation rate $R$ is nearly equal to the sum of the susceptibilities of precipitation intensity and of probability of precipitation. Consistent with previous modeling studies, the satellite retrievals reveal that precipitation susceptibility varies not only with LWP but also with $N_d$. Puzzlingly, negative values of precipitation susceptibility are found at low LWP and high $N_d$. There is marked regional variation in precipitation susceptibility values that cannot simply be explained by regional variations in LWP and $N_d$. This suggests other controls on precipitation apart from LWP and $N_d$ and that precipitation susceptibility will need to be quantified and understood at the regional scale when relating to its role in controlling possible aerosol-induced cloud lifetime effects.

## 1. Introduction

General circulation models and weather forecast models are increasingly incorporating processes by which aerosols can affect cloud properties. The effects of aerosols are represented in various ways, including impacts on cloud radiative properties and cloud microphysical processes. However, comparisons of the radiative forcing of aerosols between satellite retrieval-based estimates and global models show large disagreement, with models predicting a larger cooling effect of aerosols [*Quaas et al.*, 2009; *Boucher et al.*, 2013]. Part of the discrepancy might exist because global models inaccurately represent how precipitation depends on the cloud droplet number concentration [*Wang et al.*, 2012].

Attempts to constrain the integrated effect of aerosols on the cloud radiative properties from observations have been confounded by covariances between meteorology and aerosol conditions [*Mauger and Norris*, 2007; *George and Wood*, 2010; *Gryspeerdt et al.*, 2014]. Although efforts have been made to use conditional sampling of meteorology to isolate only the aerosol effect, concerns still exist [*Gryspeerdt et al.*, 2014]. Another approach to constrain the effect of aerosols on clouds is to examine the intermediate processes that connect aerosol changes to cloud changes [*Sorooshian et al.*, 2010].

In the cloud lifetime hypothesis proposed by *Albrecht* [1989], whereby increases in aerosol concentrations lead to increases in cloud lifetime, a crucial part of the argument hangs on the suppression of precipitation due to increases in aerosol concentrations. Previous observational studies have clearly demonstrated that precipitation from low-lying liquid clouds is suppressed by increases in aerosol and cloud droplet number concentration [*Pawlowska and Brenguier*, 2003; *Comstock et al.*, 2004; *Sorooshian et al.*, 2009; *Terai et al.*, 2012; *Mann et al.*, 2014]. Earlier studies applied a multilinear regression to all available data to obtain a single value to quantify the suppression of precipitation due to increases in aerosol concentrations [*Pawlowska and Brenguier*, 2003; *Comstock et al.*, 2004; *vanZanten et al.*, 2005], whereas the availability of more data and unique observational strategies have allowed an examination of how the suppression varies with cloud thickness [*Sorooshian et al.*, 2009; *Terai et al.*, 2012; *Mann et al.*, 2014]. The underlying goal has been to determine whether the necessary and sufficient controls that determine the suppression can be identified in order to understand

differences among various observational estimates. Our study attempts to constrain the strength of this precipitation suppression using the precipitation susceptibility metric of *Feingold and Siebert* [2009]. In addition, we attempt to understand how susceptibility varies with cloud liquid water path (LWP), because studies currently disagree on the cloud LWP dependence [*Sorooshian et al.*, 2009; *Jiang et al.*, 2010; *Terai et al.*, 2012; *Mann et al.*, 2014]. The precipitation susceptibility metric $S_R$ quantifies the fractional decrease of precipitation rate ($R$) due to a fractional increase in cloud droplet number concentration ($N_d$) [*Feingold and Siebert*, 2009]. If we define $R$ to be the mean precipitation rate averaged over an area, time period, or bin, $R$ can be decomposed into the fraction $f$ of cloud observations that are precipitating (analogous to the probability of precipitation (POP) of *Wang et al.* [2012]) and the precipitation intensity $I$ (the precipitation rate of those clouds that are precipitating). In other words,

$$R = fI. \tag{1}$$

In the susceptibility metric $S_R$, $f$ and $I$ can substitute for $R$ such that the susceptibility can take the functional form

$$S_x = -\left(\frac{\partial \ln x}{\partial \ln N_d}\right)_{\text{macro}}, \tag{2}$$

where $x$ represents $R$, $f$ (or POP), or $I$ [*Terai et al.*, 2012] and 'macro' indicates that cloud macrophysical properties are constrained to reduce the effect of covariances on quantifying the precipitation suppression due to $N_d$. Studies so far have largely only accounted for the LWP control on precipitation, whereas other controls on precipitation may exist that may act independent of LWP (e.g., turbulence [*Baker*, 1993] or giant cloud condensation nuclei [*Feingold et al.*, 1999]).

Initial studies examining the precipitation susceptibility in parcel models, satellite retrievals, and large-eddy simulations of cumulus cloud fields examined $S_I$ and noted that $S_I$ initially increases with increasing cloud LWP, reaches a peak value, and then decreases at higher LWP [*Feingold and Siebert*, 2009; *Sorooshian et al.*, 2009; *Jiang et al.*, 2010]. At the same time, steady state simple models [*Wood et al.*, 2009], aircraft observations [*Terai et al.*, 2012], and ground-based cloud radar retrievals [*Mann et al.*, 2014] have found that susceptibility monotonically decreases with increasing cloud LWP. In these studies, *Wood et al.* [2009] quantified $S_R$, whereas *Terai et al.* [2012] and *Mann et al.* [2014] both examined $S_R$ and $S_f$, where the decrease with LWP was general only in the behavior of $S_f$. Much of the difference in the behavior of susceptibility between the two sets of studies possibly lies in whether $R$, $f$, or $I$ is used to calculate the susceptibility. When the susceptibilities of the three variables $R$, $f$, and $I$ were examined in aircraft measurements, *Terai et al.* [2012] found that $S_R \approx S_f + S_I$. Because $R$ is the product of $f$ and $I$ (equation (1)) and the susceptibility takes the derivative in log space (equation (2)), when the nonlinear term capturing the covariance between $f$ and $I$ is small, the $S_f$ and $S_I$ are additive [see *Terai et al.*, 2012]. Because $S_f$ and $S_{\text{POP}}$ are the same if we aggregate both temporal and spatial variations to calculate the susceptibility, we will henceforth refer to $S_{\text{POP}}$ to stay consistent with previous studies [*Wang et al.*, 2012; *Mann et al.*, 2014]. Susceptibilities of all three aspects of the precipitation will be examined in this study.

The multimodel study of *Wang et al.* [2012] shows the possibility that the precipitation susceptibility can be used to constrain the strength of the cloud lifetime effect in climate models. The magnitude of the precipitation susceptibility metric ($S_{\text{POP}}$) and the sensitivity of LWP to aerosol concentration (dLWP/d$N$) in climate models were examined by *Wang et al.* [2012] and found to correlate, such that models with strong precipitation susceptibilities also exhibited large increases in LWP with $N$. Although the cloud lifetime effect as originally proposed specifically pointed to the increase in cloud fraction due to the suppression of precipitation [*Albrecht*, 1989], we use the term more broadly to include the increase in cloud LWP due to the suppression of precipitation. Based on the high $S_{\text{POP}}$ calculated in the default version of the Community Atmosphere Model ver.5 (CAM5) compared to the $S_{\text{POP}}$ calculated from satellite retrievals, the authors argued that the cloud lifetime effect within CAM is likely overestimated [*Wang et al.*, 2012].

In this study, we examine a set of satellite retrievals obtained from the CloudSat and Moderate Resolution Imaging Spectroradiometer (MODIS) instruments, focusing on marine stratiform clouds over the tropical and subtropical Pacific to derive the precipitation susceptibility. We specifically address the extent to which susceptibility values and behaviors across different platforms and observations can be reconciled and whether underlying commonalities exist. Section 2 introduces the CloudSat and MODIS combined data set and various methods used to calculate the precipitation susceptibility. Section 3 presents the susceptibilities

from the CloudSat and MODIS retrievals and explores the uncertainties and sensitivity of the susceptibilities to $N_d$ and regional choices. Finally, in section 4, we present a discussion and our conclusions.

## 2. Methods

### 2.1. CloudSat and MODIS Combined Data Set

The satellite retrievals used in this analysis are of warm cloud properties analyzed by *Kubar et al.* [2009, K09, hereafter] and *Wood et al.* [2009]. They pertain to 12 months of CloudSat and MODIS retrievals of cloud LWP, effective cloud droplet number concentration ($N_{\text{eff}}$), and radar reflectivity (September 2006 to February 2007 and September 2007 to February 2008) between 30°S and 30°N and between 100°E and 70°W, mostly consisting of clouds over the tropical and subtropical Pacific Ocean and Gulf of Mexico. The MAC06S0 version of the MODIS/Aqua level 2 cloud subset and the CloudSat 2B-GEOPROF data are used, and K09 found that the relationships between precipitation and cloud properties are insensitive to the months used. Given the strict criteria to screen for stratiform clouds whose microphysical retrievals are less affected by cloud edges and heterogeneities [*Zhang and Platnick*, 2011], the cloud types analyzed here are low-level marine stratiform clouds with cloud top temperatures warmer than 273 K. Of all MODIS-detected clouds in the region and during the time period, 21% of them are included in this analysis (K09). Others are not used for the following reasons. Cloud liquid water path (LWP) is retrieved using the cloud optical thickness ($\tau$) and effective radius ($r_{\text{eff}}$) (K09). $N_{\text{eff}}$, which represents an estimate of $N_d$ based on satellite retrievals, is estimated assuming the clouds are adiabatic using the method of *Bennartz* [2007; K09]. Because accurate retrievals of $N_{\text{eff}}$ cannot be made around broken clouds, data are included only if the MODIS retrievals recorded a cloud fraction of 100% in a box with sides of 5km along the satellite track and 15 km across the satellite track.

The column maximum reflectivity ($Z_{\text{max}}$) is used to infer the presence of drizzle and to estimate precipitation rate ($R$). A reflectivity threshold of −15 dBZ is used to distinguish precipitating from nonprecipitating clouds [*Comstock et al.*, 2004; *Kubar et al.*, 2009; *Terai et al.*, 2012], and a *Z-R* relationship from *Comstock et al.* [2004], based on liquid stratocumulus clouds, is used to estimate $R$ from $Z_{\text{max}}$. The *Z-R* relationship does not take into account the attenuation of $Z_{\text{max}}$ by liquid water in the cloud. Given that the clouds examined here have LWPs typically below 500 g m$^{-2}$, the effect of attenuation on the susceptibility estimates is likely small, and a sensitivity test assuming an attenuation of approximately 8 dBZ per 1000 g m$^{-2}$ of LWP [*Hogan et al.*, 2005] shows that it does not affect our susceptibility values. Assuming that the observed clouds are adiabatic particularly affects the calculation of $N_{\text{eff}}$ in the equation

$$N_{\text{eff}} = \sqrt{2}B^2\Gamma^{1/2}\frac{\text{LWP}^{1/2}}{r_{\text{eff}}^3}, \tag{3}$$

where $B = (3/4\pi\rho_w)^{1/3} = 0.0620$ and $\Gamma$ is the rate of increase of liquid water concentration with respect to height (K09). $\Gamma$ is derived from $\Gamma = f_{\text{ad}}\Gamma_{\text{ad}}$, where $\Gamma_{\text{ad}}$ is the thermodynamically determined increase of liquid water concentration for a parcel ascending adiabatically and only a function of temperature and pressure, both of which are obtained from European Centre for Medium-Range Weather Forecasts (ECMWF) reanalysis profiles of temperature and pressure. In this study, $f_{\text{ad}}$ is assumed to equal 1. With thicker clouds, precipitation and evaporative mixing reduce the ratio $\Gamma/\Gamma_{\text{ad}}$ [*Zuidema et al.*, 2005; *Rauber et al.*, 2014]. Because $\Gamma$ is not directly observable from space, we estimate the sensitivity of assuming that $f_{\text{ad}} = 1$ by also calculating the susceptibility when we use the approximation that $f_{\text{ad}} = z_0/(z_0 + z)$, where $z_0$, the cloud base height, is set to 705 m, which is the mean lifting condensation level found across the regions in the ECMWF profiles, and $z$ is the height above cloud base. In relating $N_{\text{eff}}$ to the cloud droplet number concentration $N_d$, we also assume that $r_{\text{eff}}$ is equal to the mean volume radius. We explore their potential effect on our results in section 3.1.

The analysis is constrained to warm marine stratiform clouds with optical depth greater than 3 (K09) due to MODIS retrieval uncertainties when clouds are thin or broken [*Zhang and Platnick*, 2011]. Thus, this paper does not consider the response of isolated cumulus precipitation to aerosol concentrations. Furthermore, we exclude thin clouds in the analysis and do not consider the response of midlatitude stratocumulus clouds, a large proportion of which have been found to precipitate as well [*Leon et al.*, 2008; *Muhlbauer et al.*, 2014]. However, unlike previous precipitation susceptibility studies of marine stratocumulus [*Terai et al.*, 2012; *Mann et al.*, 2014], we examine clouds over a wide geographic area with different ranges of aerosol and meteorological conditions. Because retrievals of LWP and $N_{\text{eff}}$ are only possible during the daytime, we restrict our analysis to clouds and precipitation observed ~13:30 local while acknowledging that diurnal differences in

precipitation exist and that 13:30 is near the diurnal minimum of marine stratocumulus cloud cover and precipitation rate [*Leon et al.*, 2008; *Burleyson et al.*, 2013].

### 2.2. Susceptibility Metric

The parameters that go into calculating the susceptibility can vary from study to study. For example, instead of $N_d$, the aerosol concentration ($N$), which is unavailable from space, or the aerosol index (AI) may be used [*Nakajima et al.*, 2001; *Sorooshian et al.*, 2010]. In this study, we examine the susceptibility due to variations in $N_{\text{eff}}$. Susceptibilities are typically calculated in bins of cloud LWP to control for the influence of LWP on precipitation. Different methods exist to calculate the susceptibility in each LWP bin, whether using linear regression in log-log space and using the slope to calculate susceptibility [*Sorooshian et al.*, 2010] or binning the data by $N_d$ (or $N$) and using the bin mean $N_d$ and $R$ to calculate the susceptibility [*Terai et al.*, 2012; *Wang et al.*, 2012; *Mann et al.*, 2014]. Most of the susceptibility estimates in this study are made by binning the LWP-binned data further into bins of $N_d$ and taking the linear regression of the bin mean $N_d$ and $R$, but the tercile log difference method of *Terai et al.* [2012], in which the log difference in the means of the bottom and top terciles of $N_d$ are used to calculate the susceptibility, is also used to show that they give nearly identical susceptibility values.

## 3. Results: Satellite Susceptibility

### 3.1. Basin-Wide Susceptibility as a Function of LWP

Before calculating the susceptibility, the satellite data are first binned according to LWP and $N_{\text{eff}}$ values. We divide the approximately 400,000 total CloudSat profiles into a hundred approximately equally sized bins of LWP and $N_{\text{eff}}$ bins, leaving each of the hundred [LWP, $N_{\text{eff}}$] bins with about 4000 profiles, ranging from 1200 to 5500 (middle 90th percentile of 3090–4660). In each [LWP, $N_{\text{eff}}$] bin, we calculate the bin mean precipitation metrics $R$, POP, and $I$, as well as $N_{\text{eff}}$. The susceptibility is then calculated by taking the linear regression in log space across those 10 means. We use a threshold of −15 dBZ, as in previous studies [*Comstock et al.*, 2004; *Bretherton et al.*, 2010; *Terai et al.*, 2012], to discriminate between drizzling and nondrizzling clouds. This corresponds to a precipitation rate threshold of approximately 0.14 mm $d^{-1}$ [*Comstock et al.*, 2004]. We find that $S_R$ equals approximately 0.6 at low LWP and slightly decreases to 0.5 with increasing LWP for clouds with a $N_{\text{eff}}$ range of 20 to 200 $cm^{-3}$ (Figure 1a). This is in contrast with other observational studies of stratocumulus, which found a 40% to 45% decrease in susceptibility with increasing cloud LWP [*Terai et al.*, 2012; *Mann et al.*, 2014]. The difference between the previous observational estimates, obtained in limited area studies, and the Pacific basin-wide values in Figure 1a raises the question of whether examining the susceptibilities at smaller regional scales will lead to a better agreement. Note the large error bars for the susceptibility values at low LWP. These error bars are the 95% confidence intervals in the slopes calculated by linear regression. *Feingold et al.* [2013] found that in their model analysis of a large number of parcel ensembles based on large-eddy simulations of previously observed precipitating stratocumulus and stratus clouds, susceptibility is a function not only of LWP but also of the cloud droplet number concentration $N_d$, suggesting that the log($R$) versus log($N_d$) relationship is not linear across all $N_d$, potentially leading to the wide confidence intervals at low LWP. In particular, they found that in stratocumulus and stratus clouds, the susceptibility is higher in clouds with low $N_d$. In section 3.3 we explore how susceptibility varies with $N_{\text{eff}}$.

Because $R$ is the product of POP and $I$ in each bin, $S_R$ can be approximated as the sum of $S_{\text{POP}}$ and $S_I$ [*Terai et al.*, 2012]. In other words, as in *Terai et al.* [2012], despite the wide confidence intervals at low LWP, $S_R \approx S_{POP} + S_I$, which indicates that the nonlinear covariance term between POP and $I$ is small. The implications are that we can understand the behavior of $S_R$ in terms of the magnitude and behavior of $S_{\text{POP}}$ and $S_I$. We find that $S_{\text{POP}}$ decreases with increasing LWP (Figure 1b), whereas $S_I$ *increases* with increasing LWP. The decrease of $S_{\text{POP}}$ with increasing LWP agrees with previous observational studies [*Terai et al.*, 2012; *Wang et al.*, 2012; *Mann et al.*, 2014], but the increase in $S_I$ does not. *Sorooshian et al.* [2009] and *Feingold et al.* [2013] found that $S_I$ increases with LWP in the LWP range examined in this study, from a value of 0.55 to 0.65 in *Sorooshian et al.* [2009] and from 0.6 to 0.85 in *Feingold et al.* [2013], but *Terai et al.* [2012] found that $S_I$ increased negligibly, with a constant value of 0.5. The qualitative behavior of $S_I$ here is not inconsistent with that of *Sorooshian et al.* [2009] and *Feingold et al.* [2013], but the values of $S_I$ differ substantially.

The negative $S_I$ values at low LWP in Figure 1 are especially difficult to explain in the context of our current understanding of how $N_d$ affects warm rain processes. What Figure 1 implies is that at LWP < 150 g $m^{-2}$, increasing $N_d$ decreases the frequency of precipitation (positive $S_{\text{POP}}$) but increases the intensity (negative $S_I$). To test whether this is an artifact of the method by which we calculate susceptibility, we use the

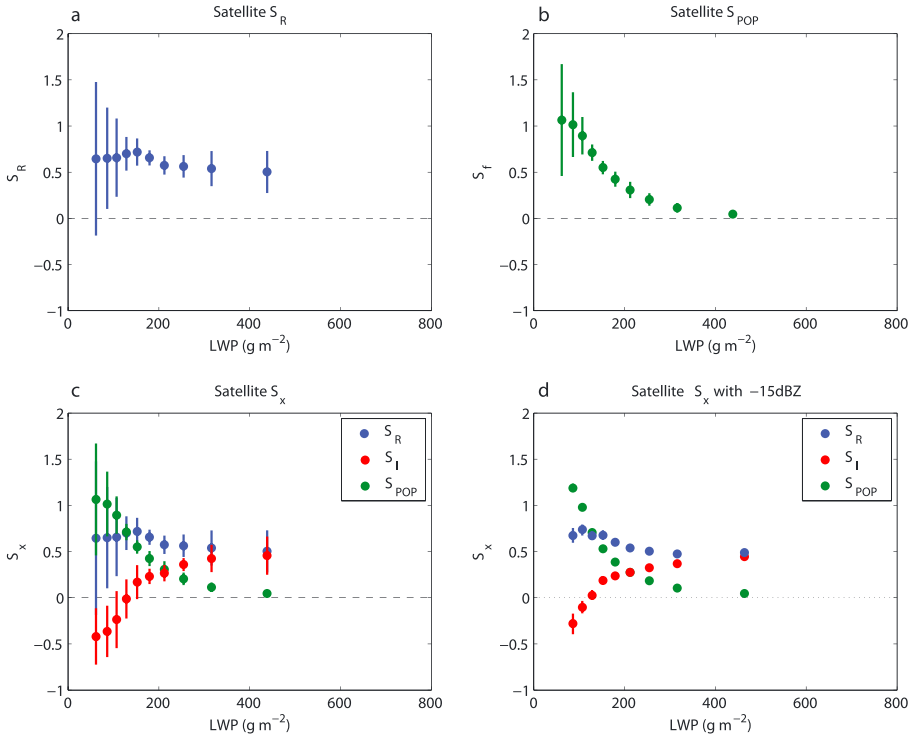


**Figure 1.** (a) Susceptibility of mean precipitation rate ($S_R$) as a function of LWP, based on the satellite data and calculated using linear regression on $N_{eff}$-binned data. (b) Susceptibility of probability of precipitation ($S_{POP}$) as a function of LWP, based on the same data and method. (c) $S_R$, susceptibility of precipitation intensity $S_I$, and $S_{POP}$ as a function of LWP, based on the same data and method. (d) $S_R$, $S_I$, and $S_{POP}$, based on the same data, but using the TLD method to calculate susceptibilities [*Terai et al.*, 2012].

tercile log-differencing (TLD) method used by *Terai et al.* [2012] to calculate the susceptibility in Figure 1d and still find similar behaviors for $S_R$, $S_{POP}$, and $S_I$. We also examined whether covariances existed between $N_{eff}$ and other cloud properties that may explain the negative $S_I$, such as cloud top height and $r_{eff}$, but found none.

Various assumptions go into deriving the susceptibility estimates. Now we discuss the potential impacts of those assumptions and uncertainties in the retrievals on the susceptibility estimates. To derive a precipitation rate from the reflectivity, we have used the *Z*-*R* relationship from *Comstock et al.* [2004]. Others exist, such as the relationship from *vanZanten et al.* [2005], which predicts a weaker dependence of *R* on *Z*. The choice of *Z*-*R* has a small effect on $S_R$ (<0.06), because it only affects the estimates of *I*, not of POP, and the effect on $S_I$ is to reduce its magnitude by approximately 15%. Related to the precipitation, we also assume that precipitation scavenging has a negligible effect when quantifying the effect of $N_{eff}$ on *R*, rather than the effect of *R* on $N_{eff}$. With typical precipitation rates of 2 mm $d^{-1}$ and a cloud droplet concentration of 50 $cm^{-3}$, the parameterization of cloud drop scavenging rate from *Wood* [2006] gives a scavenging rate of 3 $cm^{-3}$ $h^{-1}$. Given an approximate lifetime of a drizzle cell of 2 h [*Comstock et al.*, 2005], the effect would be to reduce $N_d$ by approximately 10% over the lifetime of the cloud. We expect to find the effect to be larger in heavier precipitating clouds, given that the fractional reduction from coalescence scavenging in $N_d$ scales with *R* in the parameterization [*Wood*, 2006]. Since *R* is generally higher in clouds with low $N_d$, the potential effect of the precipitation scavenging would likely be a low bias of the susceptibility values on the order of 0.1. This potential bias is on par with the statistical uncertainty represented by the sampling confidence intervals.

Another assumption that is made in relating $N_{eff}$ to $N_d$ is that the ratio between $r_{eff}$ and the mean volume radius is 1. We assume the ratio of 1, because we are unable to retrieve the ratio without knowledge of the drop size distribution. Past measurements show that this can lead to underestimating the true $N_d$ by up to 20% in more polluted clouds [*Brenguier et al.*, 2013]. The maximum potential effect on the susceptibility will be a positive bias in the susceptibility by 0.2, if the ratio changes systematically with $N_d$.

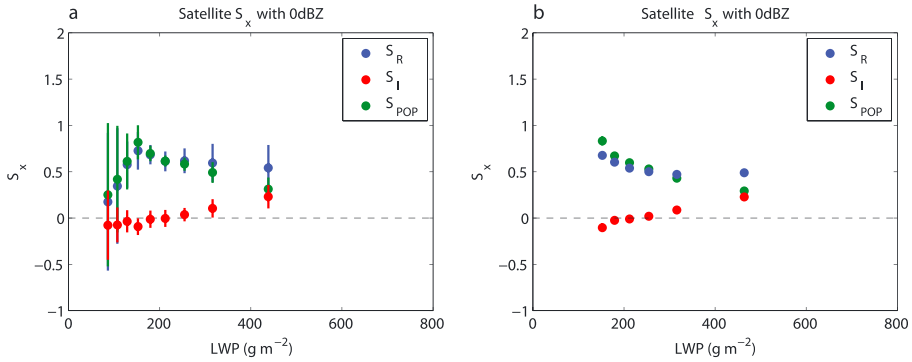


**Figure 2.** (a) $S_R$, $S_I$, and $S_{POP}$ as a function of LWP, as in Figure 1c, but using a threshold of 0 dBZ to distinguish precipitating clouds. (b) Same as Figure 2a, but using the TLD method [*Terai et al.*, 2012].

Finally, the assumption of an adiabatic cloud has possible implications. As noted by K09, if a parameterization found to approximate the adiabaticity of clouds is used on the MODIS retrievals used here, the subadiabatic $N_{eff}$ ranges from 51% of the adiabatic value in the thickest of clouds over the Asian Coast to 68% of the adiabatic values in the thinnest of clouds over the far southeast Pacific. Therefore, these values may have a substantial effect on the susceptibility values, especially if covariances exist between the thickness of the cloud and $N_{eff}$. When we compare the $S_R$ using the adiabatic and subadiabatic $N_{eff}$ values, we find that the general effect of using subadiabatic $N_{eff}$ is to shift all the $N_{eff}$ values in a LWP bin to lower values but not to largely alter the slope by which the susceptibilities are calculated. Susceptibility values are larger, generally on the order of 0.1, when the subadiabatic $N_{eff}$ is used. However, the general results of the study remain unchanged.

### 3.2. The 0 dBZ Threshold

Previous studies have examined the susceptibility by using a different reflectivity threshold than the −15 dBZ that we have used [*Sorooshian et al.*, 2009; *Wang et al.*, 2012; *Mann et al.*, 2014]. We examine how changing the threshold changes our results. The 0 dBZ threshold is a more meaningful threshold if one is interested in surface precipitation, given that cloud base precipitation with −15 dBZ rarely reaches the surface due to subcloud evaporation [*Comstock et al.*, 2004]. In Figure 2, we plot the susceptibility as a function of LWP using a minimum threshold of 0 dBZ.

Increasing the minimum threshold decreases $S_I$ to near-zero values across all LWP, and $S_R$ values mostly correspond to $S_{POP}$ values. Based on the *Z-R* relationship of *Comstock et al.* [2004] a 0 dBZ threshold corresponds to approximately 2 mm $d^{-1}$. The implication of the near-zero $S_I$ values is that heavy drizzle intensity is not susceptible to aerosols. $S_{POP}$, and hence also $S_R$, decreases for clouds with LWP < 150 g $m^{-2}$, while the $S_{POP}$ values at higher LWP remain little changed.

At first glance, $S_R$ and $S_{POP}$ calculated using linear regression and the TLD method appear to disagree (Figure 2a versus Figure 2b). The susceptibilities in the first four LWP bins are not calculated using the TLD method because less than 10% of the data points in the upper tercile of $N_{eff}$ are found to be precipitating with the new threshold. If we only compare those bins where the two methods report values, the values agree within uncertainty. Likewise, if we only compare the susceptibilities using the −15 dBZ threshold and 0 dBZ threshold where more than 10% of the data points in the upper tercile of *N* are found to be above the 0 dBZ threshold (LWP > 150 g $m^{-2}$), we note that the $S_R$ values are similar even though the $S_{POP}$ and $S_I$ values disagree (Figure 2a versus Figure 2b). This is mostly in agreement with *Mann et al.* [2014] who examined the sensitivity of results to changing thresholds and found little change in $S_R$, although *Terai et al.* [2012] found that susceptibilities can be sensitive to choice of threshold. The susceptibilities calculated by *Sorooshian et al.* [2009] and *Gettelman et al.* [2013] correspond to $S_I$ of this study, and the near-zero $S_I$ values for LWP < 300 g $m^{-2}$ in Figure 2 do not agree with either study's estimates. Given that $S_I$ is sensitive to the thresholds used, it is perhaps not surprising that the values disagree. This shows the difficulties of comparing $S_I$ across different observational platforms. From the analysis here and from *Mann et al.* [2014], $S_R$ appears to be a metric that is more robust to threshold choice.

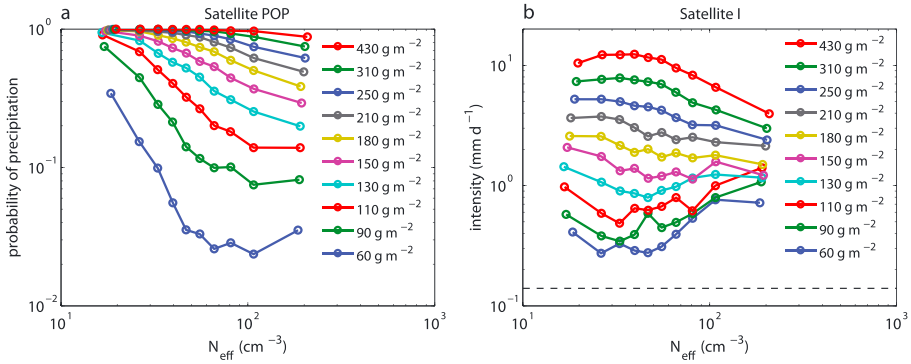


**Figure 3.** (a) Probability of precipitation (POP) and (b) precipitation intensity ($I$) as a function of effective cloud droplet number concentration ($N_{eff}$). Each line corresponds to the relationship in a particular LWP bin. The dashed line represents the precipitation equivalent of the −15 dBZ threshold used.

### 3.3. Susceptibility as a Function of LWP and $N_{eff}$

As we mentioned in section 3.1, the $\log R$ versus $\log N_{eff}$ relationship, especially at low LWP, is not linear (see Figure 3a). As a result, we see particularly large error bars in the susceptibility values at low LWP in Figure 1a. The large range of LWP and $N_{eff}$ retrievals in the combined MODIS/CloudSat data set allows us to examine the variation in susceptibility as a function of $N_{eff}$, in addition to LWP. We calculate the susceptibility at each LWP and $N_{eff}$ bin by using three consecutive $N_{eff}$ bins, rather than the full range of $N_{eff}$. We might expect large uncertainties in the susceptibilities that we calculate from the slopes calculated from a linear regression of only three points, but this method allows us to better see whether there are systematic changes in susceptibility with $N_{eff}$. In previous sections we have found that $S_I$ is negative for clouds with low LWP (Figure 1c). We can examine this issues in more detail by considering how susceptibility varies with $N_{eff}$.

$S_R$ (Figure 4a), $S_{POP}$ (Figure 4b), and $S_I$ (Figure 4c) are plotted as a function of LWP and $N_{eff}$ from the satellite data. We find that $S_R$ is highest at low LWP and low $N_{eff}$ and decreases with increasing LWP and $N_{eff}$, such that susceptibilities are zero or negative in clouds that are thin and polluted (low LWP/high $N_{eff}$) and thick and clean (high LWP/low $N_{eff}$). This pattern largely mimics that of $S_{POP}$. By comparing Figure 4b and Figure 4c, we can see that $S_I$ is largest at slightly higher LWP and lower $N_{eff}$ compared to where $S_{POP}$ maximizes.

As shown in Figure 4c, negative values of $S_I$ in Figure 1b largely occur in low-LWP/high-$N_{eff}$ clouds. As stated previously, negative $S_I$ is difficult to conceptually understand. One may hypothesize that the proximity of mean $I$ in low-LWP clouds to the minimum threshold of −15 dBZ, shown as a dashed line in Figure 3b, leads to statistical uncertainty in $I$ and to a spurious increase of $I$ with increasing $N_{eff}$. However, given that each bin has approximately 4000 data points and probability of precipitation is at least 2%, there are at least 80 profiles that contribute to the mean $I$. Furthermore, the increase of $I$ across four of the lowest LWP bins in Figure 3b suggests a structural feature in the data, where an unconsidered environmental factor that increases $I$ positively correlates with $N_{eff}$. For example, *Baker* [1993] found that precipitation formation was enhanced by stronger turbulence. If in-cloud turbulence is enhanced in more polluted clouds, this may potentially lead to increased precipitation. Although we may speculate about the sources of this odd behavior, we do not have an adequate and testable explanation. Further investigation is necessary to understand what artifacts or mechanisms may lead to the negative values of $S_I$.

### 3.4. Regional Differences

We acknowledge that $N_{eff}$ and LWP are not the only controls on precipitation rate [*Baker*, 1993; *Feingold et al.*, 1999]. *L'Ecuyer et al.* [2009] found that if they further binned their data by the lower tropospheric stability (LTS), in addition to LWP and aerosol index (AI), the proxy they used for aerosol concentration, the probability of precipitation for clouds with LWP > 500 g m$^{-2}$ was greater in stable conditions, regardless of high or low aerosol conditions. We have tried to account for stability regimes by exclusively analyzing marine stratiform clouds, which occur most frequently under stable lower tropospheres [*Klein and Hartmann*, 1993], but our susceptibility results may still be affected by mixing different LTS regimes. Therefore, we examine the susceptibility metric in different regions of the tropical/subtropical Pacific and Gulf of Mexico to determine whether the value and behavior of the susceptibility varies by region. This will also allow us to see whether the

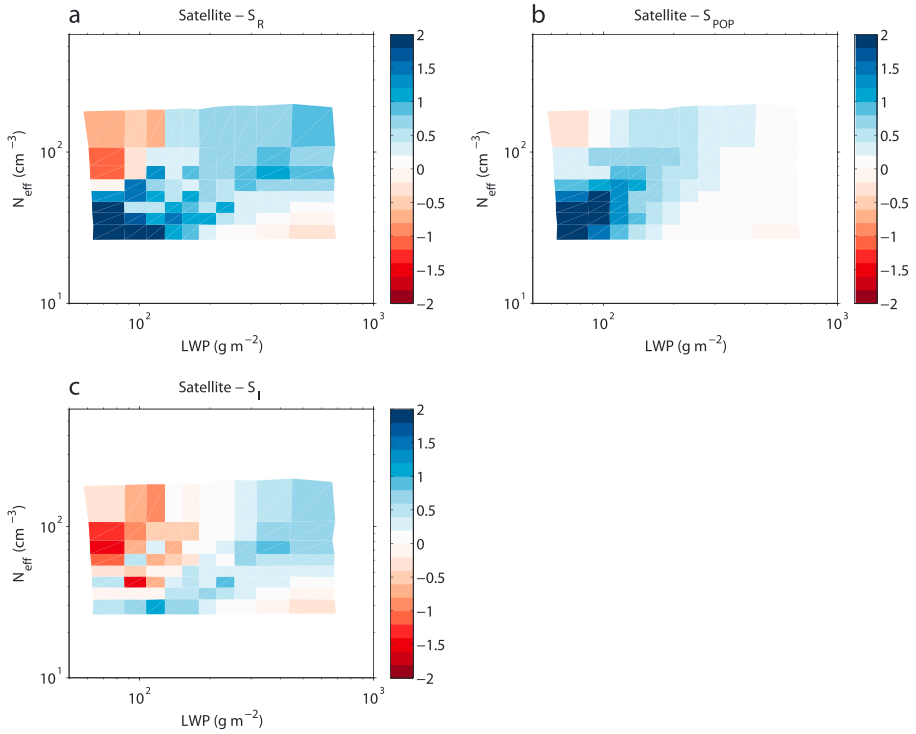


**Figure 4.** Susceptibility as a function of LWP and $N_{eff}$ calculated from linear regression of three adjacent $N_{eff}$ bins. (a) $S_R$, (b) $S_{POP}$, and (c) $S_I$ from the satellite data.

negative $S_I$ values at low LWP are found across all regions or whether it is a signal that grows out of including a particular region in the basin-wide analysis.

In Figure 5, we examine $S_R$, $S_{POP}$, and $S_I$ in seven regions, which largely correspond to the regions identified by K09. We have not examined the Intertropical Convergence Zone and South Pacific Convergence Zone, where deep convective clouds dominate. The far southeast Pacific area is modified from that defined by K09 to encompass the area sampled during the VAMOS Ocean-Cloud-Atmosphere-Land Study Regional Experiment (VOCALS-REx) [*Terai et al.*, 2012; *Mechoso et al.*, 2014]. These seven regions encompass different aerosol and meteorological regimes. For example, compared to the other regions, the Asian coast has a much higher mean $N_{eff}$ due to continental influences and also a higher LWP, compared to the remote southeast Pacific (SEP) (K09). Similar to the susceptibility that we estimate based on all of the data, the susceptibilities here are estimated from binning the data in each region by LWP and $N_{eff}$ and then taking linear regression of the binned data. Instead of the 100 total bins of [LWP, $N_{eff}$] used to calculate the susceptibility in the total data, the data in each region are binned into 25 total bins of [LWP, $N_{eff}$] such that the same number of profiles exists in each bin.

We summarize the regional mean susceptibility values found across the various regions in Table 1. Whereas the global mean $S_R$ value is approximately 0.6, the regional values range from 0.5 to 1.6. The highest $S_R$ values are found over the VOCALS southeast Pacific (SEP) region and far northeast Pacific (NEP) region. These two regions are also where $S_{POP}$ maximizes. Comparing the susceptibility values with the regional mean LWP and $N_{eff}$ values, we note that the highest $S_{POP}$ values tend to occur where the regional mean LWP are lowest, while the lowest $S_{POP}$ values occur where LWP are highest. This is consistent with the decrease in $S_{POP}$ with increasing LWP in Figure 1. The $S_I$ values do not have as strong a correspondence with regional mean LWP values, although the highest regional mean $S_I$ values are found in regions where LWP is higher. We may then ask whether we may use the regional distribution of LWP and $N_{eff}$ and the susceptibility values from Figure 4 to accurately estimate the regional mean susceptibility values. These derived estimates are reported in brackets next to the regional mean susceptibilities in Table 1. Contrary to expectations, we find that knowing the regional LWP and $N_{eff}$ distributions and the basin-wide behavior of susceptibilities as a function of LWP and $N_{eff}$ cannot help us predict the regional susceptibility values.

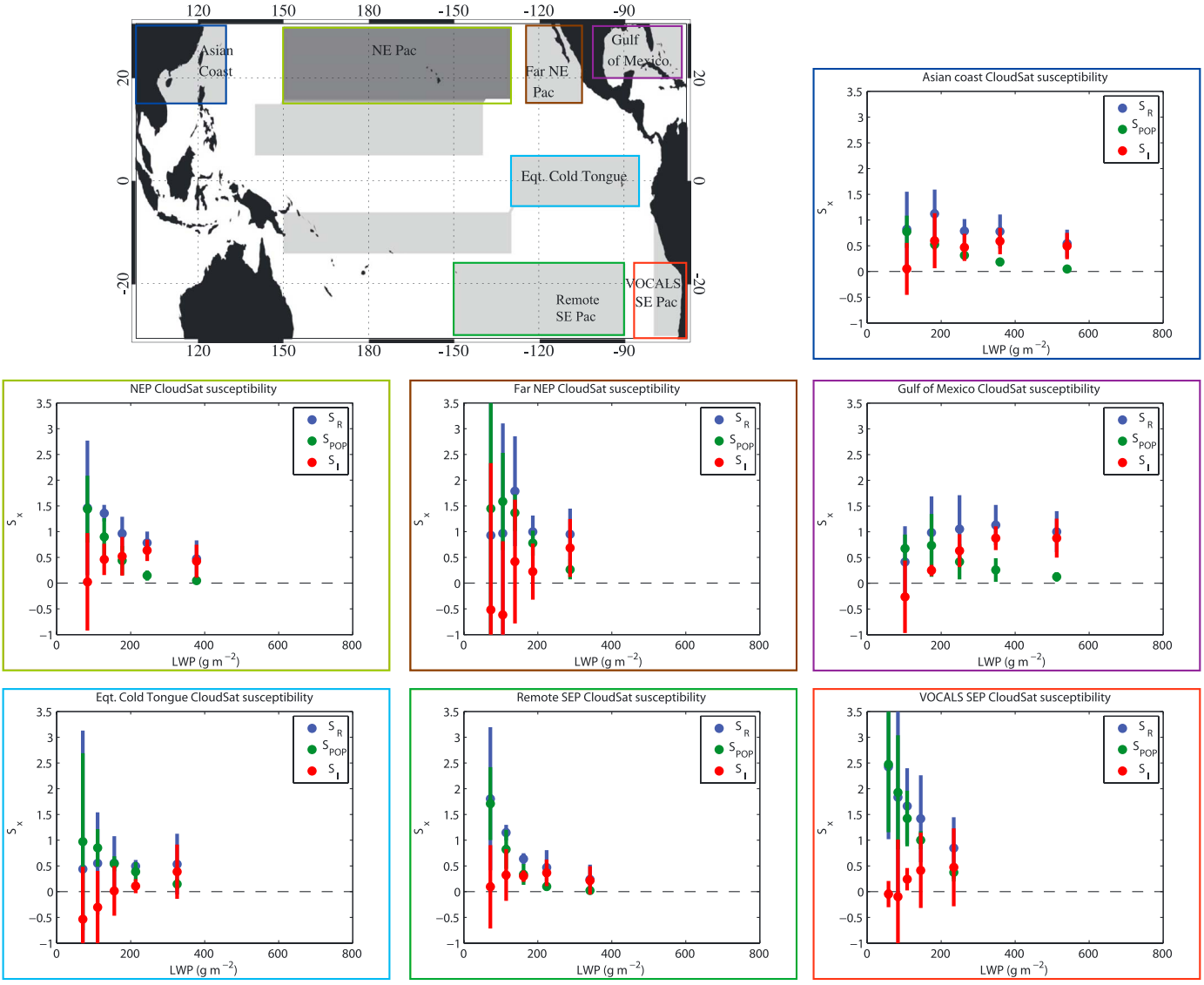


**Figure 5.** $S_R$, $S_{POP}$, and $S_I$ as a function of LWP in seven different ocean basins: Asian coast, northeast Pacific, far northeast Pacific, Gulf of Mexico, equatorial cold tongue, remote southeast Pacific, and VAMOS Ocean-Cloud-Atmosphere-Land Study (VOCALS) southeast Pacific. (Adapted from *Kubar et al.* [2009], used with permission. ©American Meteorological Society.)

From regional mean values, we shift the focus to the behaviors of $S_R$, $S_{POP}$, and $S_I$ across different regions. We find a wide variety of behaviors which highlights how susceptibilities based on measurements made in one region will not necessarily agree with those from a different region. At the same time, however, consistent behaviors do appear. For example, $S_{POP}$ across all regions decreases with increasing LWP. In addition, it appears that $S_I$ increases with increasing LWP. Whether the increase is large and at what LWP that increase occurs vary by region. Furthermore, at low LWP, $S_I$ is statistically indistinguishable from zero. Therefore, the negative $S_I$ at low LWP is not a general feature of the satellite data. $S_R$ has the most diversity across the regions and is largely determined by the addition of $S_I$ and $S_{POP}$ behaviors, as in the Gulf of Mexico, where the increase in $S_I$ is larger than the decrease in $S_{POP}$ at low LWP, leading to an increase in $S_R$ with LWP. We are therefore left with strong confidence in the general decrease of $S_{POP}$ with increasing LWP, but we find that the behavior and value of $S_R$ are more variable across regions and dependent on the behavior and value of $S_I$.

We expect the susceptibilities calculated over the VOCALS southeast Pacific region, just off the coast of South America, to agree with susceptibilities calculated by *Terai et al.* [2012]. Because the geographic regions over which they are calculated are the same, this provides a rough comparison of what different observational

**Table 1.** Mean LWP, Effective Cloud Droplet Number Concentration ($N_{eff}$), and Susceptibility Values Across Different Regions[a]

| Region | LWP (g m$^{-2}$) | $N_{eff}$ (cm$^{-3}$) | $S_R$ | $S_{POP}$ | $S_I$ |
|---|---|---|---|---|---|
| Asian coast | 290 [107, 540] | 199 [41, 444] | 0.6 [0.6] | 0.4 [0.3] | 0.6 [0.3] |
| Equatorial Cold Tongue | 175 [70, 325] | 69 [29, 127] | 0.5 [0.7] | 0.5 [0.7] | −0.1 [−0.0] |
| Far northeast Pacific (NEP) | 158 [73, 257] | 83 [32, 163] | 1.1 [0.5] | 1.1 [0.5] | 0.0 [−0.1] |
| Gulf of Mexico | 277 [102, 512] | 171 [30, 404] | 0.9 [0.6] | 0.9 [0.6] | 0.5 [0.2] |
| NEP | 202 [83, 378] | 52 [20, 101] | 1.6 [0.6] | 1.0 [0.6] | 0.4 [0.1] |
| Remote southeast Pacific (SEP) | 183 [72, 341] | 37 [17, 68] | 0.9 [0.8] | 0.6 [0.7] | 0.3 [0.1] |
| VOCALS SEP | 126 [58, 234] | 73 [25, 151] | 1.6 [0.6] | 1.4 [0.8] | 0.2 [−0.2] |

[a]The geographic extent of each region may be found in Figure 5. Next to the regional mean values of LWP and $N_{eff}$, the range (10th and 90th percentile values) are reported in brackets. After the regional mean susceptibility values, the susceptibility values estimated from applying the susceptibilities in Figure 4 to the distribution of LWP and $N_{eff}$ in each region are noted in brackets.

platforms can have on the susceptibility values. First, $S_R$ values from Figure 9 of *Terai et al.* [2012] agree with the values found in the southeast Pacific VOCALS region in Figure 5. The sharp decrease in $S_{POP}$ with increasing LWP is also observed in both results. Indeed, the susceptibilities found over the southeast Pacific VOCALS region agree better with the results of *Terai et al.* [2012] than do the susceptibilities in Figure 1 that were estimated using all of the available data. However, the increase in $S_I$ with increasing LWP, found in Figure 5, is not found in the results of *Terai et al.* [2012]. In particular, although the $S_I$ values at LWP ~200 g m$^{-2}$ agree between the two estimates, at LWP < 100 g m$^{-2}$, the satellite data here suggest an $S_I$ ~0, whereas the results of *Terai et al.* [2012] suggest a value of 0.5. Although not shown in *Terai et al.* [2012], we should note that $S_I$ slightly increases (from 0.5 to 0.7) with LWP in the range of LWP that they examined. Part of this discrepancy may be due to sampling differences between the satellite and aircraft radar retrievals. For example, the footprint of the CloudSat profiles is approximately 1.7 km by 1.3 km in the horizontal, while they are approximately 100m in the aircraft data. *Terai et al.* [2012] found that the averaging length can lead to differences in susceptibility of up to 0.5, although the change in susceptibility with averaging length was not monotonic. Most of the observations from *Terai et al.* [2012] were also obtained during late-night/early-morning flights, whereas the satellite observations are approximately from 13:30 local time. In addition, in this analysis we examine the susceptibility to changes in $N_d$, whereas *Terai et al.* [2012] examined the susceptibility to changes in accumulation-mode aerosol concentrations. Comparisons between the satellite and aircraft of radar reflectivities as functions of LWP and $N_d$ will be necessary to better understand why this discrepancy exists.

## 4. Discussion and Conclusions

In this study we examine the precipitation susceptibility metric in marine stratiform clouds over the tropical and subtropical Pacific Ocean and Gulf of Mexico. The combined MODIS/CloudSat data set gives us the opportunity to quantify the susceptibility as a function of cloud droplet number concentration and to examine how it varies by region, in order to determine whether any underlying features of the sensitivity of precipitation to aerosols can be generally understood.

Following on previous studies [*Sorooshian et al.*, 2009; *Jiang et al.*, 2010; *Terai et al.*, 2012; *Wang et al.*, 2012; *Mann et al.*, 2014], we first calculate the susceptibility as a function of LWP, using all of the available data. Large uncertainties exist in the susceptibility values. Despite the large uncertainty values, we find that $S_R$ can still be represented as a sum of $S_I$ and $S_{POP}$. Whereas $S_I$ and $S_{POP}$ are quite sensitive to the choice of precipitation threshold, $S_R$ is less sensitive, because $S_{POP}$ increases and $S_I$ decreases, essentially compensating each other, when the threshold is increased.

The wide range of LWP and $N_{eff}$ in the satellite data allow us to examine $S_R$ as a function of not only LWP but also of $N_{eff}$. $S_R$ varies as a function of $N_{eff}$, with maximum values where $S_{POP}$ values are largest. Not surprisingly, the relative contribution of $S_I$ increases as $S_{POP}$ decreases with the increase in POP. Unfortunately, we are unable to adequately explain the negative values of $S_I$ at low LWP but can identify that the negative values occur in low-LWP clouds with higher $N_{eff}$ (Figure 4). Given that the negative values of $S_I$ run counter to our existing understanding of how precipitation responds to increases in cloud droplet number concentrations and that

they do not always occur in the regional susceptibilities, further inquiry into the CloudSat radar profiles of thin, polluted clouds is necessary to determine whether it is indeed a physical feature, controlled by factors such as turbulence or giant cloud condensation nuclei, or an artifact of our satellite retrievals.

Because LWP and $N_{eff}$ distributions vary across different regions, we expect that susceptibilities also vary by region. Indeed, we find that this is the case, but even given the regional differences in susceptibilities, they still cannot explain the discrepancy between the $S_{POP}$ values from *Wang et al.* [2012] and the values in this study and others [*Terai et al.*, 2012; *Mann et al.*, 2014]. Although various regional differences exist, the notable difference between the two sets of studies is the use of AI, as opposed to $N_{eff}$. The use of AI requires retrievals of clear-sky aerosol optical depth, whereas the $N_{eff}$ retrievals require overcast clouds. Thus, the results of *Wang et al.* [2012] tend to preferentially select clouds with lower cloud cover than this study. Second of all, AI is a column integrative measure, whereas $N_{eff}$ is a volume concentration retrieval based on cloud top $r_{eff}$ of cloud drops. These differences may affect the susceptibility values in ways that are yet to be fully explored. Ideally, this issue can be reconciled using satellite field data that allow both AI and $N_d$ estimates.

Because the regional susceptibilities vary, the susceptibility in one region may not inform us about the susceptibility in another region. Although we attempted to identify the minimum set of controls that control the value and behavior susceptibility by examining the response of susceptibility to $N_{eff}$, we found that knowing the range of the LWP and $N_{eff}$ in each region cannot be used to explain regional differences. The implication of this result is that there are additional controls on susceptibility beyond LWP and $N_d$ that will need to be identified before we may arrive at an understanding that connects regional susceptibility estimates to global estimates. Identifying these additional controls may also shed light on the negative $S_l$ values found for thin, polluted clouds. Until those controls are identified, susceptibility needs to be estimated at the regional level.

Likewise, the large-eddy simulation study of *Lebo and Feingold* [2014] finds that the relationship between the cloud lifetime effect and $S_{POP}$ differs by cloud regime. In other words, increasing $S_{POP}$ in one region leads to an increase in cloud LWP, while in another region it leads to a decrease in cloud LWP. The variety of values of $S_{POP}$ and the response of clouds to $S_{POP}$ across regions suggest that it is unlikely that global $S_{POP}$ provides strong constraint on how clouds respond to aerosol perturbations in the real world, despite apparently doing so in the model world. Since the precipitation susceptibility is more easily quantified using observations compared to process rates, such as autoconversion and accretion, a deeper understanding of the processes controlling susceptibility and its effects on clouds is necessary.

**Acknowledgments**

Funding for this work was provided by NSF grant AGS-1242639 and NASA grant NNX13AQ35G (CloudSat and CALIPSO Science Team). The authors would like to thank Chris Bretherton and Sandra Yuter for valuable feedback on earlier versions of the manuscript. The authors would also like to thank the three anonymous reviewers for constructive comments that have substantially helped focus and improve the manuscript. C.R.T.'s work at LLNL was supported by the Lawrence Livermore National Laboratory (LLNL) Institutional Postdoctoral Program and conducted under the auspices of the U.S. Department of Energy by Lawrence Livermore National Laboratory under contract DE-AC52-07NA27344. The MODIS MAC06S0 product may be obtained from the Goddard Earth Science Data and Information Services Center (http://disc.sci.gsfc.nasa.gov/datacollection/MAC06S0_v2.html), whereas the CloudSat 2B-GEOPROF product may be obtained from the CloudSat Data Processing Center (http://www.cloudsat.cira.colostate.edu/). Specific data displayed in figures and data may be obtained by contacting the corresponding author (terai1@llnl.gov).

## References

Albrecht, B. A. (1989), Aerosols, cloud microphysics, and fractional cloudiness, *Science*, *245*(4923), 1227–1230.

Baker, M. B. (1993), Variability in concentrations of cloud condensation nuclei in the marine cloud-topped boundary layer, *Tellus*, *45B*, 458–472.

Bennartz, R. (2007), Global assessment of marine boundary layer cloud droplet number concentration from satellite, *J. Geophys. Res.*, *112*(D2), D02201, doi:10.1029/2006JD007547.

Boucher, O., et al. (2013), Clouds and Aerosols, in *Climate Change 2013: The Physical Science Basis. Contribution of Working Group I to the Fifth Assessment Report of the Intergovernmental Panel on Climate Change*, edited by T. Stocker, Cambridge Univ. Press, New York.

Brenguier, J.-L., et al. (2013), Radiative properties of boundary layer clouds: Droplet effective radius versus number concentration, *J. Atmos. Sci.*, *57*, 803–821.

Bretherton, C. S., et al. (2010), Southeast Pacific stratocumulus clouds, precipitation and boundary layer structure sampled along 20°S during VOCALS-REx, *Atmos. Chem. Phys.*, *10*(21), 10,639–10,654, doi:10.5194/acp-10-10639-2010.

Burleyson, C. D., et al. (2013), Ship-based observations of the diurnal cycle of southeast Pacific marine stratocumulus clouds and precipitation, *J. Atmos. Sci.*, *70*(12), 3876–3894, doi:10.1175/JAS-D-13-01.1.

Comstock, K. K., et al. (2004), Reflectivity and rain rate in and below drizzling stratocumulus, *Q. J. R. Meteorol. Soc.*, *130*(603), 2891–2918, doi:10.1256/qj.03.187.

Comstock, K. K., C. S. Bretherton, and S. E. Yuter (2005), Mesoscale variability and drizzle in southeast Pacific stratocumulus, *J. Atmos. Sci.*, *62*(10), 3792–3807, doi:10.1175/JAS3567.1.

Feingold, G., and H. Siebert (2009), Cloud aerosol interactions from the micro to the cloud scale, in *Clouds in the Perturbed Climate System: Their Relationship to Energy Balance, Atmospheric Dynamics, and Precipitation*, edited by J. Heintzenberg and R. J. Charlson, pp. 319–338 Strüngmann Forum Reports, MIT Press, Cambridge, Mass.

Feingold, G., et al. (1999), The impact of giant cloud condensation nuclei on drizzle formation in stratocumulus: Implications for cloud radiative properties, *J. Atmos. Sci.*, *56*(24), 4100–4117, doi:10.1175/1520-0469(1999)056<4100:TIOGCC>2.0.CO;2.

Feingold, G., et al. (2013), On the relationship between cloud contact time and precipitation susceptibility to aerosol, *J. Geophys. Res. Atmos.*, *118*(18), 10,544–10,554, doi:10.1002/jgrd.50819.

George, R. C., and R. Wood (2010), Subseasonal variability of low cloud radiative properties over the southeast Pacific Ocean, *Atmos. Chem. Phys.*, *10*(8), 4047–4063, doi:10.5194/acp-10-4047-2010.

Gettelman, A., et al. (2013), Microphysical process rates and global aerosol-cloud interactions, *Atmos. Chem. Phys.*, *13*(19), 9855–9867, doi:10.5194/acp-13-9855-2013.

Gryspeerdt, E., P. Stier, and D. G. Partridge (2014), Satellite observations of cloud regime development: The role of aerosol processes, *Atmos. Chem. Phys.*, *14*(3), 1141–1158, doi:10.5194/acp-14-1141-2014.

Jiang, H., G. Feingold, and A. Sorooshian (2010), Effect of aerosol on the susceptibility and efficiency of precipitation in warm trade cumulus clouds, *J. Atmos. Sci.*, *67*(11), 3525–3540, doi:10.1175/2010JAS3484.1.

Hogan, R. J., N. Gaussiat, and A. J. Illingworth (2005), Stratocumulus liquid water content from dual-wavelength radar, *J. Atmos. Oceanic Technol.*, *22*(8), 1207–1218, doi:10.1175/JTECH1768.1.

Klein, S. A., and D. L. Hartmann (1993), The seasonal cycle of low stratiform clouds, *J. Clim.*, *6*(8), 1587–1606, doi:10.1175/1520-0442(1993)006<1587:TSCOLS>2.0.CO;2.

Kubar, T. L., D. L. Hartmann, and R. Wood (2009), Understanding the importance of microphysics and macrophysics for warm rain in marine low clouds. Part I: Satellite observations, *J. Atmos. Sci.*, *66*(10), 2953–2972, doi:10.1175/2009JAS3071.1.

Lebo, Z. J., and G. Feingold (2014), On the relationship between responses in cloud water and precipitation to changes in aerosol, *Atmos. Chem. Phys.*, *14*, 11,817–11,831, doi:10.5194/acp-14-11817-2014.

L'Ecuyer, T. S., et al. (2009), Global observations of aerosol impacts on precipitation occurrence in warm maritime clouds, *J. Geophys. Res.*, *114*(D9), 1–15, doi:10.1029/2008JD011273.

Leon, D. C., Z. Wang, and D. Liu (2008), Climatology of drizzle in marine boundary layer clouds based on 1 year of data from CloudSat and Cloud-Aerosol Lidar and Infrared Pathfinder Satellite Observations (CALIPSO), *J. Geophys. Res.*, *113*, D00A14, doi:10.1029/2008JD009835.

Mann, J. A. L., et al. (2014), Aerosol impacts on drizzle properties in warm clouds from ARM Mobile Facility maritime and continental deployments, *J. Geophys. Res. Atmos.*, *119*(7), 4136–4148, doi:10.1002/2013JD021339.

Mauger, G. S., and J. R. Norris (2007), Meteorological bias in satellite estimates of aerosol-cloud relationships, *Geophys. Res. Lett.*, *34*(16), 1–5, doi:10.1029/2007GL029952.

Mechoso, C. R., et al. (2014), Ocean-cloud-atmosphere-land interactions in the southeastern Pacific: The vocals program, *Bull. Am. Meteorol. Soc.*, *95*(3), 357–375, doi:10.1175/BAMS-D-11-00246.1.

Muhlbauer, A., I. L. McCoy, and R. Wood (2014), Climatology of stratocumulus cloud morphologies: Microphysical properties and radiative effects, *Atmos. Chem. Phys.*, *14*(13), 6695–6716, doi:10.5194/acp-14-6695-2014.

Nakajima, T., et al. (2001), A possible correlation between satellite-derived cloud and aerosol microphysical parameters, *Geophys. Res. Lett.*, *28*(7), 1171–1174, doi:10.1029/2000GL012186.

Pawlowska, H., and J.-L. Brenguier (2003), An observational study of drizzle formation in stratocumulus clouds for general circulation model (GCM) parameterizations, *J. Geophys. Res.*, *108*(D15), 1–13, doi:10.1029/2002JD002679.

Quaas, J., et al. (2009), Aerosol indirect effects—General circulation model intercomparison and evaluation with satellite data, *Atmos. Chem. Phys.*, *9*(22), 8696–8717, doi:10.5194/acp-9-8697-2009.

Rauber, R. M., et al. (2014), Rain in shallow cumulus over the ocean: The RICO campaign, *Bull. Am. Meteorol. Soc.*, *88*(12), 1912–1928, doi:10.1175/BAMS-88-12-1912.

Sorooshian, A., et al. (2009), On the precipitation susceptibility of clouds to aerosol perturbations, *Geophys. Res. Lett.*, *36*(13), 1–5, doi:10.1029/2009GL038993.

Sorooshian, A., et al. (2010), Deconstructing the precipitation susceptibility construct: Improving methodology for aerosol-cloud precipitation studies, *J. Geophys. Res.*, *115*, D17201, doi:10.1029/2009JD013426.

Terai, C. R., et al. (2012), Does precipitation susceptibility vary with increasing cloud thickness in marine stratocumulus?, *Atmos. Chem. Phys.*, *12*(10), 4567–4583, doi:10.5194/acp-12-4567-2012.

vanZanten, M. C., et al. (2005), Observations of drizzle in nocturnal marine stratocumulus, *J. Atmos. Sci.*, *62*( 1), 88–106, doi:10.1175/JAS-3355.1.

Wang, M., et al. (2012), Constraining cloud lifetime effects of aerosols using A-Train satellite observations, *Geophys. Res. Lett.*, *39*(15), 3–9, doi:10.1029/2012GL052204.

Wood, R. (2006), Rate of loss of cloud droplets by coalescence in warm clouds, *J. Geophys. Res.*, *111*, D21205, doi:10.1029/2006JD007553.

Wood, R., T. L. Kubar, and D. L. Hartmann (2009), Understanding the importance of microphysics and macrophysics for warm rain in marine low clouds. Part II: Heuristic models of rain formation, *J. Atmos. Sci.*, *66*(10), 2973–2990, doi:10.1175/2009JAS3072.1.

Zhang, Z., and S. Platnick (2011), An assessment of differences between cloud effective particle radius retrievals for marine water clouds from three MODIS spectral bands, *J. Geophys. Res.*, *116*, D20215, doi:10.1029/2011JD016216.

Zuidema, P., et al. (2005), Ship-based liquid water path estimates in marine stratocumulus, *J. Geophys. Res.*, *110*, D20206, doi:10.1029/2005JD005833.